

Black-hole bubbles

I. G. Moss

Department of Theoretical Physics, University of New Castle, Newcastle upon Tyne, NE1 7RU, England,

(Received 23 October 1984)

If theories of high-energy physics such as spontaneous symmetry breaking and quantum chromodynamics are correct, then exploding black holes will be surrounded by phase-transition bubbles or fireballs, supported by the pressure of particles trapped inside a high-temperature phase. For quark-gas fireballs, where there is a hadron bag with a hole in it, this enhances the γ -ray emission by a factor of 69 which could lead to a feature in the γ -ray background around 200 MeV. For other bubbles there may be detectable electromagnetic pulses produced by the Rees mechanism when the bubble bursts, particularly for the inflated bubbles which result from the models suggested by the inflationary-universe scenario.

I. INTRODUCTION

Modern theories of high-energy physics predict the existence of phase transitions,¹ some of them at temperatures higher than are likely to be obtainable in the laboratory. Since the opportunities to test such theories are so limited it becomes of interest to consider the effects of such theories on the behavior of primordial black holes, that is, black holes produced in the very early universe, which we might hope to observe astronomically.

A black hole of mass M radiates energy due to the well-known Hawking effect,² characterized by a temperature of

$$T_h = (8\pi M)^{-1} \quad (1)$$

in dimensionless units such that $\hbar=c=G=k=1$. As the black hole evaporates, the temperature rises and we have the possibility that a bubble of a high-temperature phase surrounds the horizon. This process is resisted by the inward pressure of the low-temperature phase which resists the growth of the high-temperature phase inside the bubble, and if the black hole can heat up a large enough region we will see only a fireball, somewhere in the middle of which is the exploding black hole. For the case of Higgs-Kibble³ models of fundamental interactions, for example, there should be a restoration of symmetry at high temperatures with an associated phase transition. However, Hawking has shown that for exploding black holes the high-temperature region would be too localized and symmetry would not be restored.⁴

We shall consider a new effect that arises when some particles emitted by the black hole are reflected from the wall of a bubble. Such particles will be referred to as "trapped particles" in what follows. For example, in the case of the Higgs-Kibble models, symmetry breaking is associated with the presence of particles which are massless in the symmetric phase but which have a nonzero rest mass m in the broken-symmetry phase. These particles can be emitted by the black hole into a bubble of the restored-symmetry phase, but those with energy less than m would have imaginary momentum outside of the bubble and must therefore be trapped. Another case of this

new effect is for the quark model of hadrons where results suggest that there exists a deconfined or weakly interacting quark-gas phase of matter⁵ at high temperatures. While a black hole can happily radiate quarks into such a phase, the quarks are then trapped within it because of the well-known fact that free quarks do not exist.

The extra pressure on the bubble wall resulting from these reflected particles pushes the bubble surface outward. Because the dynamical time scale for these effects is usually much shorter than the evaporation time of the black hole, the bubble wall reaches equilibrium at a point where the forces upon it are balanced. We shall see in Sec. II that this point lies at a minimum of an effective free energy which can be constructed from the latent heat of the symmetric phase, the surface tension of the bubble wall, and an effective pressure inside of the bubble. This thermodynamic viewpoint allows us to consider situations such as a quark-gas fireball, where the underlying theoretical model is not so well understood, in Sec. V.

The calculation of the effective pressure inside of the bubble requires a knowledge of quantities such as $\langle \phi^2 \rangle$ near a black hole, which we shall take a look at in Sec. III. The presence of the bubble wall means that we are in an intermediate situation between the case of a black hole radiating into free space and a black hole in thermal equilibrium, both of which have been investigated by Candelas,⁶ and numerically by Fawcett and Whiting.⁷ The difference between the two cases lies principally in the choice of vacuum state. For a black hole in free space we must use the Unruh vacuum state⁸ which is defined with respect to regular time coordinates at past null infinity and on the past horizon of the fully extended black-hole metric. A black hole in thermal equilibrium, on the other hand, corresponds to the Hartle-Hawking⁹ vacuum state defined with respect to time coordinates which are regular on the past and future black-hole horizons. In the case that we are interested in we must use the Unruh vacuum state. However, in the limit that the transmission coefficient of the wall goes to zero we shall see in Sec. III that one recovers the results for a black hole in thermal equilibrium, just as if we had used the Hartle-Hawking state.

In most cases of interest and in the cases of most in-

terest the radius of the bubble wall is much greater than the Schwarzschild radius of the black hole and our computational task is greatly eased because we can neglect the effects of spacetime curvature. The main process which limits the size of the bubble is the loss of energy by the trapped particles interacting with particles which pass freely through the bubble wall. For broken-symmetry models this limits the large bubbles to cases where the interaction constant are small. In the case of the quark-gas fireball this scattering is mainly electromagnetic which is small enough to allow a large bubble radius.

Without a black-hole bubble the radiation emitted by an evaporating black hole is likely to be free radiation in which interactions are insignificant,¹⁰ but the black hole is not a perfect blackbody radiator due to the scattering of radiation from the curved spacetime. The luminosity is given by

$$\frac{dM}{dt} = \alpha M^{-2}, \quad (2)$$

where α is a constant. Table I shows the value of α and the remaining lifetime of a black hole for various temperatures. This table uses the emission rates calculated by Page¹¹ applied to the SU(5) grand unified theory.¹² The occurrence of black-hole bubbles will only affect the lifetime if there is a large inflow of material back into the black hole, which is unlikely. However, the nature of the radiation is very much affected. For example, the γ -ray luminosity of the hole increases by a factor of around 70 as the temperature rises through 200 MeV because the quarks which are emitted by the hole radiate energy by annihilation and bremsstrahlung processes, and this may lead to a feature in the γ -ray background.

There is evidently a wide range of energy, and an even wider range of black-hole lifetimes, above 1 GeV. Bubbles will arise whenever there is a phase transition without too many losses caused by scattering. They can appear very rapidly, giving sudden jumps in the emission spectra. They can also burst very rapidly, releasing large numbers of highly relativistic charged particle-antiparticle pairs which lead to electromagnetic pulses by the mechanism suggested by Rees.¹³ Some particular examples of this are given in Sec. VI.

II. BUBBLES

Consider a model in which a U(1) gauge symmetry is broken in flat space by the vacuum expectation value of a Higgs field ϕ . If we include a Fermi field ψ and a gauge field A_μ , then the action has the form

TABLE I. The lifetime of a black hole is given for a variety of temperatures. The luminosity parameter α (see text) is given in Planck units of 3.63×10^{59} erg sec⁻¹.

Temperature	α	Lifetime
1 MeV	3.6×10^{-4}	6.4×10^{21} sec
200 MeV	23×10^{-4}	1.1×10^{14} sec
100 MeV	41×10^{-4}	0.5×10^6 sec
10^{15} MeV	45×10^{-4}	0.3×10^{-18} sec

$$S = \int \left[-\frac{1}{2}(D\phi)^* \cdot (D\phi) - \frac{1}{4}F \cdot F - \bar{\psi} \not{D} \psi - \bar{\psi} m \psi - V_0(\phi) - f \bar{\psi} \psi \phi \right] dv, \quad (3)$$

where $F_{\mu\nu}$ is the Maxwell tensor and D_μ is the gauge-covariant derivative $D_\mu + igA_\mu$. We can take the potential $V_0(\phi)$ to be a quartic polynomial in $|\phi|$, but quantum effects lead to an effective potential $V(\phi)$ which must be of the form shown in Fig. 1 for spontaneous symmetry breaking to occur in flat space. This potential has a global minimum at the broken-symmetry value of $\phi = \phi_0$ and a local minimum at $\phi = 0$ with an energy difference ϵ^4 between them. There may also exist a potential barrier of height ξ^4 , resulting from the radiative one-loop quantum corrections, for example.

Our aim is to study semiclassical soliton solutions $\phi(r)$ where r is the radial coordinate of the black-hole metric,

$$ds^2 = - \left[1 - \frac{2M}{r} \right] dt^2 + \frac{dr^2}{(1-2M/r)} + r^2(d\theta^2 + \sin^2\theta d\phi^2). \quad (4)$$

In the usual manner⁴ we shall shift the scalar field operator to $\phi + \phi_1 + i\phi_2$ where ϕ_1 and ϕ_2 are fluctuating quantum fields with vanishing expectation values. This enables us to construct an effective action $\Gamma[\phi]$ by integrating over the quantum fields in a path integral, and to one-loop order we get⁴

$$\Gamma[\phi] = \int \left[-\phi \square \phi + V_1(\phi) \right], \quad (5)$$

where

$$V_1(\phi) = V(\phi) + \frac{1}{2}\phi^2\nu(r). \quad (6)$$

The flat-space quantum corrections are included in $V(\phi)$, but the extra black-hole effects are contained in

$$\nu(r) = g^2 \langle A^2 \rangle + f^2 \langle \bar{\psi} \psi \rangle + 3\lambda \langle \phi_1^2 \rangle + \lambda \langle \phi_2^2 \rangle, \quad (7)$$

where $\frac{1}{4}\lambda$ is the quadratic coupling constant. These expectation values depend upon the black-hole mass M and the choice of vacuum state.

A black-hole bubble solution can now be defined as a static spherically symmetric solution of the field equations

$$\square \phi = V'_1(\phi) \quad (8)$$

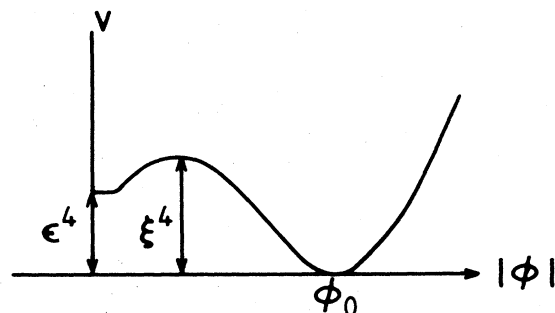


FIG. 1. A typical Higgs potential $V(\phi)$.

or more fully

$$\left[1 - \frac{2M}{r}\right] \frac{d^2\phi}{dr^2} + \frac{2}{r} \left[1 - \frac{M}{r}\right] \frac{d\phi}{dr} = V'(\phi) + v(r)\phi \quad (9)$$

which is regular on the horizon and approaches the broken-symmetry value ϕ_0 at large distances from the hole. On the horizon, ϕ will not be a regular function of r but it will be well behaved in the Kruskal coordinate system¹⁴

$$U = -e^{-(t-r)/4M} \left[\frac{r}{2M} - 1 \right]^{1/2}, \quad (10)$$

$$V = e^{(t+r)/4M} \left[\frac{r}{2M} - 1 \right]^{1/2}$$

of the completed black-hole spacetime shown in Fig. 2. At the crossing point $U=V=0$ we have

$$\frac{\partial\phi}{\partial U} \frac{\partial\phi}{\partial V} = - \left[\frac{\partial\phi}{\partial r} \right]^2 16M^2 e^{-1} (1 - 2M/r) \quad (11)$$

which must vanish for a regular solution. Therefore the boundary conditions of the bubble solution to Eq. (9) are

$$\left[1 - \frac{2M}{r}\right]^{1/2} \frac{d\phi}{dr} \rightarrow 0 \text{ as } r \rightarrow 2M, \quad (12)$$

$$\phi \rightarrow \phi_0 \text{ as } r \rightarrow \infty. \quad (13)$$

The existence of a nontrivial bubble solution depends upon the size of $v(r)$. We can argue this along the lines of Coleman's description of false vacuum decay,¹⁵ by the analogy between Eq. (9) and a mechanical particle moving in a potential $-V$. From the field equation (7) we can get an energy equation,

$$\begin{aligned} \frac{1}{2} \left[1 - \frac{2M}{r}\right] \left[\frac{d\phi}{dr} \right]^2 - V \\ = - \int_{2M}^r \frac{2}{r} \left[1 - \frac{3M}{2r}\right] \left[\frac{d\phi}{dr} \right]^2 dr \\ + \int_{2M}^r v(r)\phi \frac{d\phi}{dr} dr - V(0). \end{aligned} \quad (14)$$

The solution starts off from $r=2M$ with ϕ near the symmetric value $\phi=0$, shown in Fig. 3. Without the terms on the right, energy conservation prevents the solution reach-

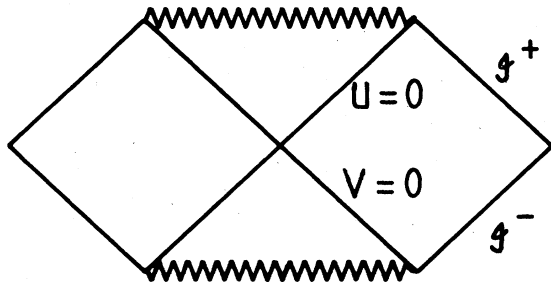


FIG. 2. The Penrose diagram of a complete black-hole spacetime.

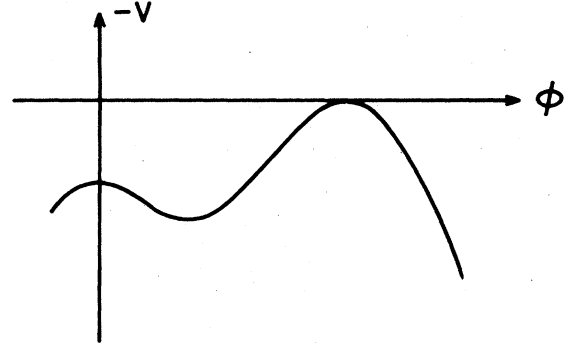


FIG. 3. The potential $-V(\phi)$.

ing the top of the hill at $\phi=\phi_0$. On the other hand, the second term increases the energy and can cause ϕ to overshoot ϕ_0 at a finite radius provided that $v(r)$ is large. If this happens, the initial value of ϕ can be reduced, which also has the effect of reducing the energy-nonconserving terms, to such an extent that ϕ does not reach $\phi=\phi_0$. Therefore there must be some intermediate starting point from which ϕ just comes to rest at $\phi=\phi_0$. This is the bubble solution.

To be of physical interest, the bubble must be stable and not collapse as time goes by. We shall examine the stability of thin-wall bubbles. These are bubbles which look like a spherical region of restored symmetry surrounded by a thin wall in which ϕ grows from zero to ϕ_0 . Denote such a solution by $\phi(r;\bar{r})$, where the position \bar{r} of the bubble wall is defined by

$$\bar{\phi}(\bar{r};\bar{r}) = \phi_1 \quad (15)$$

for some value ϕ_1 which is chosen to lie in the range zero to ϕ_0 . The bubble wall may then be perturbed to a position $\bar{r}(t)$ and the field equation (8) for the perturbed field can be used to give

$$\begin{aligned} \frac{1}{2} \left[1 - \frac{2M}{r}\right] \left[\frac{\partial\bar{\phi}}{\partial r} \right]^2 - V \\ = \int_{2M}^r \frac{\partial\bar{\phi}}{\partial r} \left[\frac{\partial^2\bar{\phi}}{\partial\bar{r}^2} \bar{r}^2 + \frac{\partial\bar{\phi}}{\partial\bar{r}} \right] \\ - \int_{2M}^r \frac{2}{r} \left[1 - \frac{3M}{2r}\right] \left[\frac{\partial\bar{\phi}}{\partial r} \right]^2 dr \\ + \int_{2M}^r v(r)\bar{\phi} \frac{\partial\bar{\phi}}{\partial r} dr - V(0). \end{aligned} \quad (16)$$

Because of the thin-wall approximation, the radial derivative of $\bar{\phi}$ is zero except near $r=\bar{r}$, and we can simplify the integrals. Furthermore, we are perturbing a stationary solution so that we may also take \bar{r} to be small. We therefore get, for $r=\infty$,

$$S_1 \ddot{\bar{r}} = -\epsilon^4 - \frac{2}{\bar{r}} \left[1 - \frac{3M}{2\bar{r}}\right] S_1 + \frac{1}{2} v(\bar{r})\phi_0^2, \quad (17)$$

where

$$S_1 = \int_{2M}^{\infty} \left(\frac{\partial \bar{\phi}}{\partial r} \right)^2 dr \tag{18}$$

is the surface action. This is the equation of motion for the bubble wall which behaves like a body with a mass S_1 per unit area. The first and second force terms represent pressure and surface-tension forces which push the wall inward towards the black hole. The third term represents an outward pressure from the medium inside the bubble.

We can best examine the equilibrium of the bubble wall by introducing an effective free energy F such that

$$4\pi\bar{r}^2 S_1 \ddot{\bar{r}} = - \frac{dF}{d\bar{r}} \tag{19}$$

Comparing this with Eq. (17), we see that

$$F(r) = \frac{4}{3}\pi r^3 \epsilon^4 + 4\pi r^2 \left[1 - \frac{3M}{2r} \right] S_1 - \frac{4\pi}{3} r^3 p(r), \tag{20}$$

where the effective pressure is defined by

$$p(\bar{r}) = \frac{3}{2\bar{r}^3} \int_{2M}^{\bar{r}} v(r) \phi_0^2 r^2 dr \tag{21}$$

Stable equilibrium then occurs at the value of \bar{r} which correspond to the minima of F . At such values increasing \bar{r} results in an inward-going force whereas decreasing \bar{r} leads to an outward-going force.

We are now in a position to construct a strategy for investigating black-hole bubbles. For any particular model we usually have a good idea of the values of ϵ^4 and S_1 . For example, if the potential has the form shown in Fig. 1 then $S_1 \simeq \frac{1}{6}\xi^2\phi_0$. The effective pressure p requires a little more effort but it can be evaluated by the methods described in the next two sections. If the resulting free energy F has a global minimum at some radius larger than the Schwarzschild radius of the black hole then a bubble solution is likely to arise. However, it can happen that a free-energy barrier prevents the growth of the bubble. In this case thermal tunneling may take place which, by analogy with thermodynamic results,¹⁶ should have a rate proportional to $e^{-F(\bar{r})/T}$ where \bar{r} is the value of the bubble radius corresponding to the top of the free-energy barrier.

The advantage of this approach is that we need not be restricted to broken-symmetry models. Other theories, such as quantum chromodynamics⁵ appear to have high-temperature phases and also surface energies on phase boundaries.

III. BLACK HOLES IN LEAKY BOXES

Let us assume that the black hole is surrounded by a thin-walled bubble whose radius is much larger than the Schwarzschild radius and that some of the particles emitted by the black hole are reflected off the bubble wall. We can treat this situation as one in which the black hole has been surrounded by a spherical box which allows some of the radiation to leak away.

We shall obtain an expression for $\langle \phi_1^2 \rangle$ in the case that

$V'''(0)$ is zero. This can easily be extended to cases where $V'''(0)$ is nonzero and to similar expressions for the other fields which enable us to calculate the effective pressure inside the bubble. The first step is to expand the quantum field ϕ in terms of suitable positive- and negative-frequency modes,

$$\phi = \sum_i (a_i p_i + a_i^\dagger p_i^*), \tag{22}$$

where the a_i are the annihilation operators of the Unruh vacuum state. These modes, defined with respect to the Kruskal V coordinate on the past horizon, are linear combinations of the mode functions^{2,17}

$$(4\pi\omega)^{-1/2} e^{\pm i\omega t} Y_{lm}(\theta, \phi) R_l(r) r^{-1} \tag{23}$$

The radial functions $R_l(r)$ themselves come in two types, distinguished by their asymptotic behavior. Outward-going modes

$$\begin{aligned} \vec{R} &= e^{i\omega r^*} + \vec{A} e^{-i\omega r^*}, \quad r^* \rightarrow -\infty \\ &= \vec{B} e^{i\omega r}, \quad r^* \rightarrow \infty \end{aligned} \tag{24}$$

where

$$r^* = r + 2M \ln \left[1 - \frac{2M}{r} \right] \tag{25}$$

are emitted from the hole with unit flux and encounter a potential barrier for which the reflection and transmission coefficients are \vec{A} and \vec{B} . On the other hand, the inward-going modes

$$\begin{aligned} \overleftarrow{R} &= \overleftarrow{B} e^{-i\omega r^*}, \quad r^* \rightarrow -\infty \\ &= e^{-i\omega r} + \overleftarrow{A} e^{i\omega r}, \quad r^* \rightarrow \infty \end{aligned} \tag{26}$$

come from outside of the hole with unit flux. We can represent these modes by diagrams such as shown in Fig. 4, in which the r^* coordinate runs from left to right and lines are used to represent the flux.

The radial functions for a black-hole bubble must allow for the mass m of the field in the broken-symmetry phase beyond the bubble wall. This causes scattering of the modes from the wall, with which we may associate reflection and transmission coefficients S and T . These new radial functions have the form

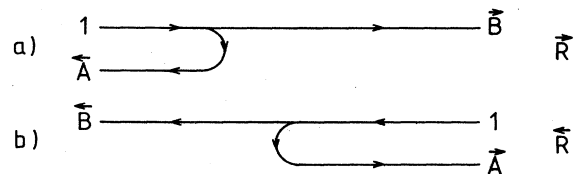


FIG. 4. Diagrammatic representation of the mode functions \vec{R} and \overleftarrow{R} . The r^* coordinate runs from left to right and lines labeled by the amplitude are used to represent the flux.

$$\begin{aligned}\vec{P} &= e^{i\omega r^*} + \vec{a} e^{-i\omega r^*}, \quad r \rightarrow 2M \\ &= \vec{b} e^{i\omega r} + \vec{c} e^{-i\omega r}, \quad r \rightarrow \bar{r} \\ &= \left[\frac{\omega}{k} \right]^{1/2} \vec{d} e^{ikr}, \quad r \rightarrow \infty\end{aligned}\quad (27)$$

$$\begin{aligned}\overleftarrow{P} &= \overleftarrow{d} e^{-i\omega r^*}, \quad r \rightarrow 2M \\ &= \overleftarrow{c} e^{i\omega r} + \overleftarrow{b} e^{-i\omega r}, \quad r \rightarrow \bar{r} \\ &= \left[\frac{\omega}{k} \right]^{1/2} (e^{-ikr} + \overleftarrow{a} e^{ikr}), \quad r \rightarrow \infty\end{aligned}\quad (28)$$

where $k^2 = \omega^2 - m^2$. The amplitudes of the various waves can be found by following through the flux in a diagram such as shown in Fig. 5. One obtains

$$\begin{aligned}\vec{a} &= BB^*{}^{-1} \frac{1 - S^* \overleftarrow{A}^*}{1 - S \overleftarrow{A}} S, \quad \vec{b} = \frac{B}{1 - S \overleftarrow{A}}, \quad \vec{c} = \frac{BS}{1 - S \overleftarrow{A}}, \\ \overleftarrow{a} &= TT^*{}^{-1} \frac{1 - \overleftarrow{A}^* S^*}{1 - \overleftarrow{A} S} \overleftarrow{A}, \quad \overleftarrow{b} = \frac{T}{1 - S \overleftarrow{A}}, \quad \overleftarrow{c} = \frac{T \overleftarrow{A}}{1 - \overleftarrow{A} S}.\end{aligned}\quad (29)$$

For $r < \bar{r}$, these radial modes are still solutions of the radial wave equation and they can therefore be expressed in terms of the original modes,

$$\vec{P} = \frac{BS}{1 - S \overleftarrow{A}} \overleftarrow{R} + \vec{R}, \quad (30)$$

$$\overleftarrow{P} = \frac{T}{1 - S \overleftarrow{A}} \overleftarrow{R}. \quad (31)$$

We may now obtain an expression for $\langle \phi^2 \rangle$ in the same way that is described in Ref. 6. After regularization, this gives

$$\begin{aligned}\langle \phi^2 \rangle &= \frac{1}{16\pi^2 r^2} \\ &\times \int_0^\infty \frac{d\omega}{\omega} \left[\sum_l (2l+1) (\coth \frac{1}{2} \beta \omega (|\vec{P}|^2 + |\overleftarrow{P}|^2)) \right. \\ &\quad \left. - \frac{4\omega^2}{1 - 2M/r} \right] \\ &- \frac{M^2}{48\pi^2 r^4} \left[1 - \frac{2M}{r} \right]^{-1},\end{aligned}\quad (32)$$

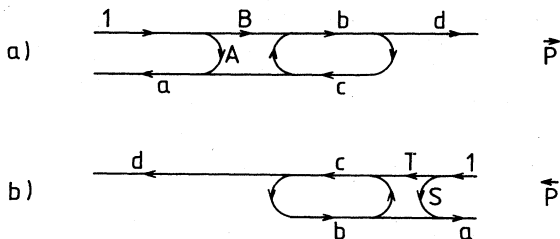


FIG. 5. Diagrammatic representation of the mode functions \vec{P} and \overleftarrow{P} .

where $\beta = 8\pi M$.

Reflection of the modes from the bubble wall will be associated with a phase shift which tends to disorder the phases of the modes and complicate the final result. We can overcome this problem in the case that the bubble wall is larger than the predominant wavelengths, $\omega \bar{r} \gg 1$, by smearing the radial dependence of $\langle \phi^2 \rangle$ which has the effect of averaging over the phase shifts.¹⁸ We can therefore replace functions of S by their average, denoted by square brackets,

$$[S] = \left[\frac{S}{1 - S \overleftarrow{A}} \right] = 0, \quad (33)$$

$$\left[\frac{1}{|1 - S \overleftarrow{A}|^2} \right] = \frac{1}{1 - |S|^2 |A|^2}.$$

Hence

$$[\vec{P}^* \vec{P}] = \frac{(1 - |A|^2) |S|^2}{1 - |S|^2 |A|^2} |\overleftarrow{R}|^2 + |\vec{R}|^2, \quad (34)$$

$$[\overleftarrow{P}^* \overleftarrow{P}] = \frac{1 - |S|^2}{1 - |S|^2 |A|^2} |\overleftarrow{R}|^2.$$

When substituted into the expression (32) for $\langle \phi^2 \rangle$, we recover the result for a black hole radiating into free space in the limit that $|S| = 0$,

$$\langle \phi^2 \rangle = \frac{1}{8\pi^2 r^2} \int_0^\infty \frac{d\omega}{\omega} \frac{\sum (2l+1) |B|^2}{e^{\beta\omega} - 1}, \quad (35)$$

and if we use the large- or small-frequency limit¹¹ $\sum (2l+1) |B|^2 \simeq 16M^2 \omega^2$ we get

$$\langle \phi \rangle^2 = 1/192\pi^2 r^2. \quad (36)$$

As $|S|$ is increased to one we find instead the result for $\langle \phi^2 \rangle$ in the Hartle-Hawking vacuum state. This is just what one expects because the black hole can come into thermal equilibrium with its surroundings.

The most important contribution to $\langle \phi^2 \rangle$ for the black-hole bubble comes from those modes with frequencies less than m which would have imaginary three-momentum k outside of the bubble and they are therefore totally reflected with $|S| = 1$. If scattering between the modes can be neglected, we have

$$\begin{aligned}\langle \phi^2 \rangle &= \frac{1}{16\pi^2 r^2} \\ &\times \int_0^m \frac{d\omega}{\omega} \left[\sum (2l+1) \coth 2\beta\omega (|\overleftarrow{R}|^2 + |\vec{R}|^2) \right. \\ &\quad \left. - \frac{4\omega^2}{1 - 2M/r} \right] - \frac{M^2}{48\pi^2 r^4} \left[1 - \frac{2M}{r} \right]^{-1},\end{aligned}\quad (37)$$

and there are similar results for $\langle A^2 \rangle$ and $\langle \bar{\psi}\psi \rangle$. Unlike the previous case (36), the value of $\langle \phi^2 \rangle$ does not decrease with increasing radius but it does increase with temperature to give a large outward pressure on the bubble wall. In fact, the potentially large size of $\langle \phi^2 \rangle$ is the essential feature which leads to the formation of black-hole bubbles.

The result of scattering on low-frequency modes is that particles in these modes can escape from the bubble and this can be more important than the curved-space effects included in (37). To handle both of these effects would require techniques such as those developed by Hawking for interacting fields near a black hole.⁴ Fortunately, as we shall see, in many cases of interest the bubble is much larger than the black hole and we can neglect the space-time curvature throughout most of the bubble interior.

IV. SCATTERING

From now on we shall consider the black hole as simply a source which is radiating into the interior of a black-hole bubble. This radiation consists of particles which interact with one another according to a Lagrangian such as the one used in Sec. II. Provided that the bubble is larger than the Compton wavelength of these particles, then the occupation numbers $N(\mathbf{x}, \mathbf{k}, \omega)$ of the various types of particles in modes of frequency ω and wave number \mathbf{k} satisfy Boltzmann's equations

$$\mathbf{k} \cdot \frac{dN}{d\mathbf{x}} = -N \int dk_1 dk_2 dk_3 (2\pi)^4 \delta(k_3 + k_2 - k - k_1) |\mathcal{T}|^2 \times \{N(k)N(k_1)[1 \pm N(k_2)][1 \pm N(k_3)] - N(k_2)N(k_3)[1 \pm N(k)][1 \pm N(k_1)]\}, \quad (38)$$

where $dk = d^3k / (2\pi)^3 (2\omega)$ and \mathcal{T} is the appropriate scattering matrix element. The plus and minus signs correspond to bosons and fermions, respectively. These equations relate the particle flux terms on the left, to the amount of scattering given by the scattering integral on the right.

We are interested in static situations where $\partial N / \partial t$ vanishes. The spherical symmetry implies that we may take

$$N \equiv N(r, \omega, \mu), \quad (39)$$

where $\mu = \cos\theta = \mathbf{x} \cdot \mathbf{k} / r\omega$. This enables us to replace the partial differential operator in the flux terms,

$$\omega \mu \frac{\partial N}{\partial r} + \omega \frac{1 - \mu^2}{r} \frac{\partial N}{\partial \mu}, \quad (40)$$

by an ordinary differential operator,

$$\omega \frac{(1 - \mu^2)}{r} \frac{dN}{d\mu}, \quad (41)$$

where the derivative is taken along the curves $r(1 - \mu^2)^{1/2} = \Gamma$, sketched in Fig. 6. However, these curves do not pass through $\theta = 0$ or $\theta = \pi$ and functions such as $\delta(\theta)$ which have support only at $\theta = 0$ must be treated separately. Consequently, Boltzmann's equations can be decomposed into equations for the $\delta(\theta)$ dependent part, which we shall call the beam, and the remainder which we shall call the medium. The beam can be thought of as radiation emitted directly from the black hole into the surrounding medium.

Let us define frequency-averaged functions $n(r, \mu)$ and $h^\pm(r)$ by

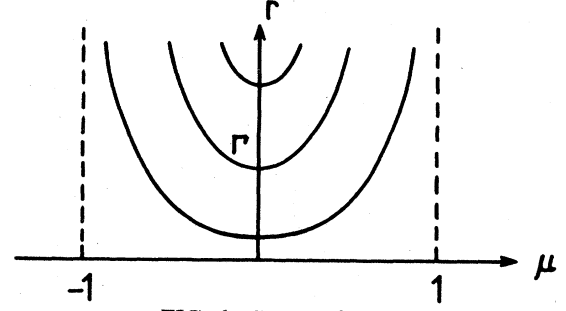


FIG. 6. Curves of constant Γ .

$$4\pi \int \frac{N\omega d\omega}{(2\pi)^3} = n + 2h + \frac{\delta(\theta)}{\sin\theta} + 2h - \frac{\delta(\theta - \pi)}{\sin\theta}. \quad (42)$$

We can then construct two angular averages. One of these is the flux,

$$f = \frac{1}{2} \int_{-1}^1 n\mu d\mu + h^+ - h^- \quad (43)$$

and the other one is the quantity which we are aiming to calculate,

$$\langle \phi^2 \rangle = 2\pi \int \frac{N\omega d\omega d\mu}{(2\pi)^3} = \frac{1}{2} \int_{-1}^1 n d\mu + h^+ + h^-, \quad (44)$$

where the scalar field ϕ could equally well be a Maxwell field A_μ or a fermion field ψ depending on the particle under consideration.

We shall construct equations for n and h in two limiting cases, one in which the particle interactions are not strong enough to thermalize the medium and another case in which they are. In the first case the beam will reach the bubble wall with the same spectral distribution that it had when it was emitted by the black hole. If the spherical symmetry was exact then the trapped particles would be reflected back into the hole. However, in more realistic situations the reflected particles will form a medium surrounding the hole. We can then find an approximate form of the Boltzmann equations related to the scattering-length approximation in statistical mechanics. This takes the form (see Appendix A)

$$\frac{1 - \mu^2}{r} \frac{dn}{d\mu} = -\kappa_1 n n_0 + \kappa_2 n_0 h, \quad (45)$$

$$\frac{dh}{dr} + \frac{2h}{r} = -\kappa_3 n_0 h, \quad (46)$$

where the κ are scattering lengths and n_0 , the lowest-order approximation to n , is much larger than h . Equation (45) represents scattering from the medium to untrapped particles and to the medium from the beam. The approximate solutions are

$$n = n_0 e^{-\kappa_1 \mu n_0 r}, \quad (47)$$

$$h = P r^{-2} e^{-\kappa_2 n_0 r}, \quad (48)$$

where P is a constant, which we can obtain from a black hole radiating into free space as given by Eq. (36),

$$P = 1/192\pi^2 \approx 1/1895. \quad (49)$$

The values of the flux and $\langle \phi^2 \rangle$ corresponding to these solutions are

$$f = -\frac{2}{3}\kappa_1 r n_0^2 + P/r^2 \quad (50)$$

and

$$\langle \phi^2 \rangle = n_0 + \frac{1}{6}(\kappa_1 r)^2 n_0^2 + P/r^2. \quad (51)$$

At the bubble wall, the flux of trapped particles must vanish but particles in the beam with frequency $\omega > m$ can still escape. We therefore have

$$f(\bar{r}) = \frac{P}{\bar{r}^2} \left[1 - \frac{I_1(m)}{I_1(\infty)} \right], \quad (52)$$

where the integral I_1 is given in Appendix A. Equating Eqs. (50) and (52) gives

$$n_0 = \left[\frac{3P_1}{2\kappa_1} \right]^{1/2} \bar{r}^{-3/2}, \quad (53)$$

where

$$P_1 = P \frac{I_1(m)}{I_1(\infty)}, \quad (54)$$

and this term dominates $\langle \phi^2 \rangle$ because our assumptions imply that κ_1 is very small. If we now recall some of the results of Sec. II, Eqs. (7), (20), and (21), we can obtain the effective free energy,

$$F = \frac{4}{3}\pi r^3 \epsilon^4 + \frac{2\pi}{3} \epsilon^2 \phi_0^2 r^2 - \frac{4}{3}\pi r^{3/2} m^2 \left[\frac{3P_1}{2\kappa_1} \right]^{1/2}, \quad (55)$$

where $m^2 = \lambda \phi_0^2$. This is sketched in Fig. 7, which shows that there is a stable equilibrium point for the bubble wall. Replacing the scalar particles with gauge fields gives the same result but with $m^2 = g^2 \phi_0^2$ and κ_1 is given by an expression familiar in form to that of Appendix A, but with λ replaced by the effective-gauge-field-interaction constant $\alpha = g^2/4\pi$.

There are two requirements for the consistency of the bubble solution in this case. First, we require that $\bar{r} \gg \beta_h/4\pi$ for the bubble to be much larger than the Schwarzschild radius of the black hole. We also require that $\kappa_2 n_0 \bar{r} < 1$, otherwise the medium will be in the thermalized condition considered below. For a Coleman-Weinberg model,¹⁹ for example, we would have $\lambda \sim \alpha^2$.

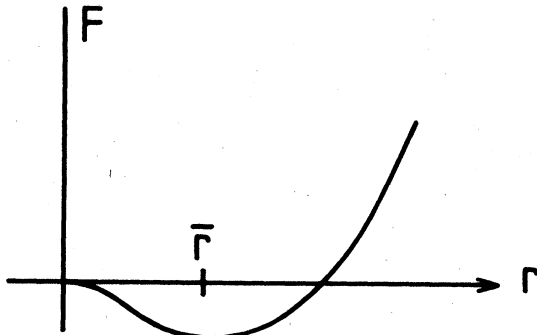


FIG. 7. The free energy of a bubble wall.

At the critical temperature $\beta^{-1} \sim m$,

$$\bar{r} \sim \alpha^{-2} m^2 \beta_h^{-1} \quad (56)$$

which is indeed much larger than the black hole. Such models are of interest because they arise in the inflationary scenario of the very early universe.²⁰

The alternative case in which the medium thermalizes at some temperature β^{-1} is considered in Appendix B. Clearly this can only happen if $\beta^{-1} < m$. We get the same simplified equations (39) and (40) as before, but now we require $\kappa_2 \gg \kappa_1$. The solution becomes

$$n = n_0 - \kappa_1 n_0^2 \mu r - \frac{\kappa_2 P n_0}{2r(1-\mu^2)^{1/2}} S \left[\theta - \frac{\pi}{2}; \kappa_2 n_0 r \sin \theta \right], \quad (57)$$

$$h = P r^{-2} e^{-\kappa_2 n_0 r}, \quad (58)$$

where $S(\theta; \lambda)$ is the Sievert integral,

$$s(\theta; \lambda) = \int_0^\theta e^{-\lambda \sec \theta'} d\theta' \quad (59)$$

and $n_0 = \frac{1}{12} \beta^{-2}$. The flux becomes

$$f = -\frac{2}{3} \kappa_1 r n_0^2 + P/r^2. \quad (60)$$

At the bubble wall, only those particles with $\omega > m$ can escape, with a flux,

$$f(\bar{r}) = I_1(\infty) \left[1 - \frac{I_1(m)}{I_1(\infty)} \right] \approx \frac{1}{4\pi^2} m \beta^{-1} e^{-\beta m}, \quad (61)$$

where we use the fact that $\beta^{-1} < m$. Comparing this with Eq. (60) gives an equation for β ,

$$\frac{C}{216} \beta^{-3} \bar{r}^3 + \frac{1}{4\pi^2} m \beta^{-1} \bar{r}^2 e^{-\beta m} = P, \quad (62)$$

where κ_1 has been replaced by its value $C\beta$ from Appendix B. For $m\bar{r} \gg (P/C)^{1/3}$ the first term dominates and we get

$$\langle \phi^2 \rangle \approx \frac{1}{12} \beta^{-2} \approx 3 \left[\frac{P}{C} \right]^{2/3} \bar{r}^{-2}, \quad (63)$$

whereas for $1 \ll m\bar{r} \ll (P/C)^{1/3}$ we get

$$\langle \phi^2 \rangle \approx \frac{1}{12} \beta^{-2} \approx \frac{m^2}{12} \left[\ln \frac{4\pi^2 P}{m^2 \bar{r}^2} \right]^2. \quad (64)$$

As in the previous case we can construct an effective free energy using the results of Sec. II. In the large \bar{r} limit this has the form

$$F = \frac{4}{3}\pi r^3 \epsilon^4 + 4\pi r^2 S - 6\pi r m^2 \left[\frac{P}{C} \right]^{2/3} \quad (65)$$

which is very similar to the one sketched in Fig. 7.

The consistency of a bubble solution in this case again requires $\bar{r} \gg \beta_h/4\pi$, which can be viewed as an upper limit on the scattering constant C . We also require $\kappa_2 n_0 \bar{r} > 1$ for thermalization.

V. QUARK FIREBALLS

Let us assume that strong interactions are described by quantum chromodynamics,⁵ which predicts that quarks and gluons are confined to color-singlet states such as baryons and mesons. This theory is asymptotically free, which means that the strength of the quark interactions decreases with energy. In fact, both analytic investigations and lattice-theory calculations⁵ predict that the theory undergoes a phase transition to a weakly interacting gas phase above a critical temperature $T_c \approx 200$ MeV or for distances less than the "flux-tube radius" $\bar{a} \approx 5 \times 10^{-14}$ cm.

So far we have examined black-hole bubbles for models with spontaneous broken symmetries. There are very similar models for hadrons, known as the bag models,²¹ which are meant to reproduce the behavior of quantum chromodynamics at a phase transition in a manner analogous to Ginzberg-Landau theory in statistical mechanics. Such models produce good agreement, often to within 10%, with the observed properties of many baryons and mesons. We shall concentrate on a particular example due to Freidberg and Lee,²² which includes several other bag models as special cases.

The volume energy density or latent heat ϵ^4 of the quark-gas phase can be related to the phase-transition temperature as follows. Suppose that the gas inside a large spherical box is at a temperature T . The free energy is then given by Eq. (20), with an effective pressure

$$P = \frac{1}{24} T^2 \bar{m}^2, \quad (66)$$

where

$$\bar{m}^2 = \sum (g^2 \phi_0^2 + f^2 \phi_0^2 + \lambda \phi_0^2) \quad (67)$$

and the sum extends over all the particle degrees of freedom. At the critical temperature this balances the ϵ^4 term and we must therefore have

$$\epsilon^4 = \frac{1}{24} T_c^2 \bar{m}^2. \quad (68)$$

In the bag-model approximation, this mass \bar{m} is responsible for confining the quarks inside color-singlet states and it must therefore be chosen to be as large as possible. It is, however, an unphysical parameter that we shall try to eliminate.

We can obtain an expression for the surface energy S from the mass of a typical baryon. The results of Ref. 22 show that about one third of the baryon mass is made up of the energy of the scalar field. For a flavor-averaged baryon mass m_b of around 1.3 GeV, we get an expression

$$\frac{4}{3} \pi r_p^3 \epsilon^4 + 4 \pi r_p^2 S = \frac{1}{3} m_b, \quad (69)$$

where r_p is the proton radius, $r_p \approx 5.4 m_b^{-1}$.

A black-hole bubble now becomes a black hole inside a bag. The trapped particles are, of course, the quarks and gluons which cannot escape because of color confinement. They should still interact strongly enough even in the gaseous phase inside the bubble to come into equilibrium. They can, however, scatter energy into nontrapped particles because of electromagnetic interactions and the main loss mechanisms are shown in Fig. 8.

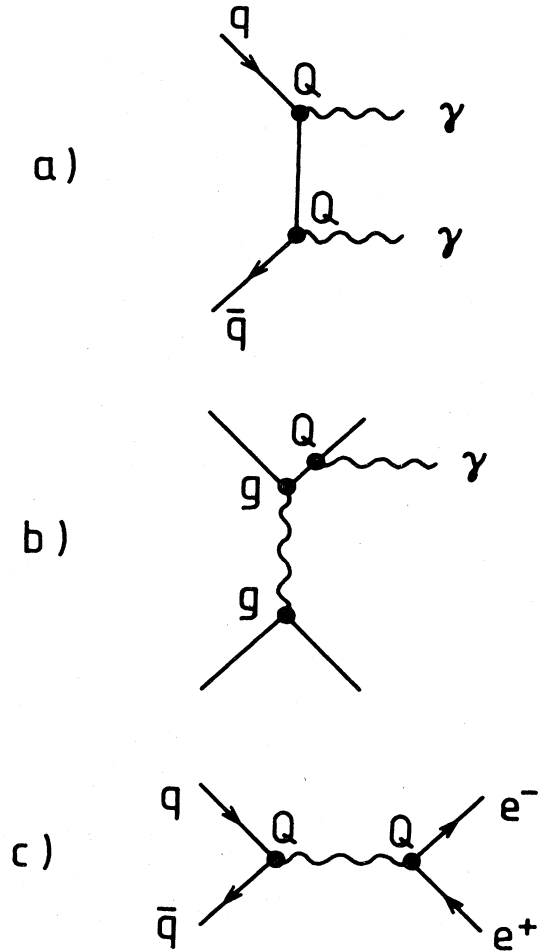


FIG. 8. Feynman diagrams for the principal energy loss mechanisms of a quark-gas bubble.

The first process produces γ rays from the pair annihilation of quarks. We can construct the corresponding element $|\mathcal{T}|^2$ by the usual diagrammatic techniques.²³ It is sufficiently accurate for our purposes to replace $|\mathcal{T}|^2$ by an average over the center-of-mass scattering angle ψ , and we obtain

$$|\mathcal{T}|^2 = 4Q^4 \ln \frac{2}{\beta^2 m_q^2} \quad (70)$$

to leading order in βm_q , where Q and m_q are the charge and mass of the quark. A similar expression can be obtained for the bremsstrahlung process, but this depends upon the strong-interaction constant g . For now, let us assume that the resulting expression is smaller than the annihilation result (70). Finally, the pair production process gives

$$|\mathcal{T}|^2 = \frac{1}{3} Q^2 e^2,$$

where e is the charge of the electron. Therefore, under our assumptions, the energy loss is dominated by pair annihilation of the lightest quark. We shall take $m_q \approx 20$ MeV, but the particular value will have only a very weak effect on the final result.

The free energy of the bubble is given by Eq. (65) of the previous section, with

$$C = \frac{5 \times 2^4 \pi^4}{3^5 \xi(3)} \left[\frac{e^2}{4\pi} \right]^2 f(0) \quad (71)$$

which follows from replacing λ^2 by $|\mathcal{F}|^2$ in the result of Appendix B. The minimum of the free energy corresponds to a stable bubble wall at

$$\bar{r} = \left[\left(\frac{S}{\epsilon^4} \right)^2 + \left(\frac{P}{C} \right)^{2/3} \frac{24}{T_c^2} \right]^{1/2} - \frac{S}{\epsilon^4}, \quad (72)$$

where Eq. (61) has been used to eliminate ϵ^4 . This value of the radius depends upon \bar{m} through the quantity S/ϵ^4 . However, for large values of \bar{m} the volume term dominates the free energy and \bar{r} is independent of \bar{m} ,

$$\bar{r} \approx \sqrt{24} \left(\frac{P}{C} \right)^{1/3} T_c^{-1} \approx 20 f^{-1/3} T_c^{-1}. \quad (73)$$

This is consistent with our assumption that the bubble is much larger than the Schwarzschild radius $1/r\pi T$.

We therefore expect that as the temperature of the black hole rises above T_c it will become surrounded by a quark-gas fireball, radiating mostly γ rays. However, highly energetic quarks can penetrate the bubble wall by distorting it outwards into a flux tube, the breakup of which leads to a shower of pions and other hadrons. Such events are known as jets and they are common features of high-energy-physics experiments. Gibbons²⁴ *et al.* have investigated the occurrence of these jets in black-hole explosions, and they should be important once the black-hole temperature has risen above 1 GeV.

VI. ASTROPHYSICAL CONSEQUENCES

We shall consider just two effects of black-hole bubbles which may be relevant to the observation of black-hole explosions. The first is the effect of an enhanced γ -ray emission from the quark-gas fireball upon the γ -ray background, and the second is the possibility that unstable bubbles may emit electromagnetic pulses.

The luminosity of a black hole is given by

$$\frac{dM}{dt} = \alpha M^{-2}, \quad (74)$$

where we shall take $\alpha = \alpha_1$ for black-hole temperatures below T_c and $\alpha = \alpha_2$ for temperatures above T_c . The γ -ray component of the luminosity will be denoted by γ_1 and γ_2 . Following Carter *et al.*¹⁰ we shall take a power-law distribution for the number of black holes in a comoving volume,

$$dN = AM^2 M_i^{-4-\epsilon} dM, \quad (75)$$

where M is the mass of a black hole at a time t and M_i is the mass of the same black hole at the recombination time t_i . Such a black hole will radiate predominantly at a frequency $(8\pi M)^{-1}$ but this radiation will be red-shifted so that today, $t = t_1$, it will contribute to the background radiation at a frequency of

$$\nu = \frac{1}{8\pi M} \left(\frac{t}{t_1} \right)^{2/3}. \quad (76)$$

It follows that the total contribution from all of the black holes radiating at the time t to the γ -ray energy density today is

$$d\rho = \frac{\gamma AM_i^{-4-\epsilon}}{8\pi} \left(\frac{t}{t_1} \right)^{4/3} \frac{d\nu}{\nu^2} dt, \quad (77)$$

where dM has been eliminated in favor of $d\nu$. The initial mass M_i can be expressed as a function of ν and t by integrating the mass-loss equation (74),

$$M_i^3 = 3\alpha_1(t - t_i) + M^3, \quad t > t_c \quad (78)$$

$$M_i^3 = 3\alpha_i(t - t_i) + M_c^3 + \frac{\alpha_1}{\alpha_2}(M^3 - M_c^3), \quad t < t_c \quad (79)$$

where

$$t_c = \left(\frac{\nu}{T_c} \right)^{3/2} t_1 \quad (80)$$

is the time at which the temperature of the black hole was T_c .

A very good approximation to ρ can be obtained by replacing the mass terms in equations (78) and (79) with M_c^3 . For the frequency range of interest, one then finds

$$\begin{aligned} d\rho &\approx \frac{3A\gamma_1}{8\pi} \frac{1}{3-\epsilon} t_1 M_1^{-2-\epsilon} \frac{d\nu}{\nu^2} \\ &\quad + \frac{3A\gamma_2}{8\pi} \frac{1}{3-\epsilon} t_1 M_1^{-2-\epsilon} \left(\frac{\nu}{T_c} \right)^{(3-\epsilon)/2} \frac{d\nu}{\nu^2}, \quad \nu < T_c \\ &\approx \frac{3A\gamma_2}{8\pi} \frac{1}{3-\epsilon} t_1 M_1^{-2-\epsilon} \frac{d\nu}{\nu^2}, \quad \nu > T_c \end{aligned} \quad (81)$$

where $M_1^3 = 3\alpha_1 t_1$ corresponds to a black hole whose lifetime equals the age of the universe t_1 . For $\nu \ll T_c$, the result is very similar to the one given by Carter *et al.*, with a frequency spectrum proportional to ν^{-2} . This is also true for $\nu > T_c$, but the constant of proportionality increases by a factor $\gamma_2/\gamma_1 \simeq 69$ as a result of the increase in γ -ray emission from the quark fireball which forms at $T = T_c$.

The observed limit on the energy density in the γ -ray background for a few MeV is around $10^{-37} \text{ g cm}^{-3}$. This leads to the condition $AM_1^{-2-\epsilon} < 8 \times 10^{-169}$, corresponding to a present-day limit of around 10^4 black holes per cubic pc, which is very similar to the conclusion of earlier work.^{25,26} However, the spectrum (81) has an additional feature that we could, in principal, also determine ϵ independently of A by examination of the slope of the spectrum when $\nu \simeq T_c$.

Let us now turn to the prospects for observing the effects of high-energy symmetry restoration near a black hole due to the breakup of a black-hole bubble. This may occur after the black hole vanishes, with the bubble hiding away the ultimate fate of the black hole. Alternatively, a bubble can suddenly become thermodynamically favorable or just as suddenly unfavorable and disappear depending

upon the relative heights of the minima of the effective free energy. A bubble will therefore eventually burst, releasing a large quantity of energy. Rees¹³ has shown that such sudden releases of energy produce electromagnetic pulses due to the interaction of charged particle-antiparticle pairs with the ambient galactic magnetic field.

The amount of energy available in the low-scattering bubble of Sec. IV is roughly

$$E \sim \frac{4\pi}{3} \bar{r}^3 n_0 \beta_h^{-2} \sim \alpha^{-6} m \quad (82)$$

for a black-hole temperature β_h^{-1} . A significant fraction may be converted into charged-particle pairs, leading to a pulse with a characteristic wavelength

$$\lambda \sim \left[\frac{6E}{B^2} \right]^{1/3} \left[\frac{\bar{m}}{m} \right]^{8/3}, \quad (83)$$

where \bar{m} is the rest mass of the charged particle and B is the magnitude of the galactic magnetic field, typically around 5×10^{-6} Gauss. Thus

$$\lambda \sim 10^3 \alpha^{-2} \left[\frac{m}{1 \text{ GeV}} \right]^{1/3} \left[\frac{m}{\bar{m}} \right]^{-8/3} \text{ cm}. \quad (84)$$

The number of detectable photons is largest when λ corresponds to energies far below m , and this is more likely to be the case for proton-antiproton pairs rather than electron-positron pairs. A bubble bursting at energies above 100 GeV with α of order the fine-structure constant gives a radio pulse which is easily detectable from 10^{15} cm away. For larger energy-phase transitions the value of α would have to be very small to give an observable effect. However, values of α as small as 10^{-4} have been considered in the context of inflationary models of the very early universe.^{20,27} Such a bubble at a temperature of 10^{10} GeV could produce a great many γ -ray photons of energy around 1 MeV. The expanding ball of protons would reach nearly 10^{10} cm giving a pulse duration of around 1 sec. These events would have to be close by to be detectable and they would therefore show no tendency towards lying in the plane of the galaxy.

ACKNOWLEDGMENTS

This work began as a result of a suggestion by Stephen Hawking that phase transitions near a black hole might be of interest. I would like to express my gratitude to him for encouragement, and to Don Page for helpful discussions. This work was supported by the Science and Engineering Research Council.

APPENDIX A

We wish to simplify the Boltzmann equation (38) for a weakly interacting scalar field. This can be extended to other fields in a similar way. Consider a scalar field which corresponds to trapped particles for frequencies less than m , and which couples by four-line vertex interactions to an untrapped field, with coupling constant λ_1 and to itself with coupling constant λ_2 , as shown in Fig. 9. The occupation number N for trapped modes of the scalar field can be decomposed, as discussed in Sec. IV, into

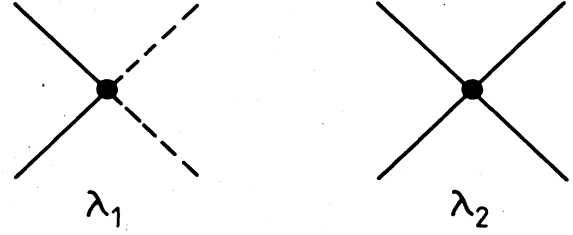


FIG. 9. Interaction terms for a trapped field (solid line) and an untrapped field (broken line).

medium N_m and beam N_b parts. These have a blackbody form

$$N_m = \frac{f(\mu, r)}{e^{\beta_h \omega} - 1}, \quad \omega < m \quad (A1)$$

$$N_b = \frac{12\beta_h^2 h(r)}{e^{\beta_h \omega} - 1} \frac{\delta(\theta)}{\sin\theta}, \quad \omega < \infty \quad (A2)$$

where $12\beta_h^2 h \ll f \ll 1$ and β_h^{-1} is the black-hole temperature. The occupation numbers of any untrapped modes will be negligible compared to 1 far from the black hole.

The Boltzmann equation has the form

$$\mathbf{k} \cdot \frac{dN}{d\mathbf{x}} = \xi, \quad (A3)$$

where ξ is the scattering integral,

$$\begin{aligned} \xi = & \int dk_1 dk_2 dk_3 (2\pi)^4 \delta(k_2 + k_3 - k - k_1) \\ & \times [-\lambda_1^2 N(k)N(k_1) - \lambda_2^2 N(k)N(k_1) \\ & + \lambda_2^2 N(k_2)N(k_3)]. \end{aligned} \quad (A4)$$

This decomposes into medium and beam terms ξ_m and ξ_b where

$$\begin{aligned} \xi_m = & -\lambda_1^2 \int dk_1 dk_2 dk_3 N_m(k)N_m(k_1) \\ & \times (2\pi)^4 \delta(k_2 + k_3 - k - k_1), \end{aligned} \quad (A5)$$

$$\begin{aligned} \xi_b = & -\lambda_2^2 \int dk_1 dk_2 dk_3 N_b(k)N_m(k_1) \\ & \times (2\pi)^4 \delta(k_2 + k_3 - k - k_1). \end{aligned} \quad (A6)$$

Hence

$$\begin{aligned} 4\pi \int \frac{\omega d\omega}{(2\pi)^3} \xi_m & = -\lambda_1^2 4\pi \int \frac{\omega d\omega}{(2\pi)^3} 4\pi \int \frac{\omega_1 d\omega_1}{(2\pi)^3} \\ & \times \int \frac{d\tilde{\mu}}{16\pi} N_m(k)N_m(k_1) \\ & \approx -\frac{\lambda_1^2}{8\pi} n(\mu)n_0, \end{aligned} \quad (A7)$$

where

$$n_0 = \frac{1}{2} \int_{-1}^1 n d\mu \quad (A8)$$

and $\tilde{\mu}$ is the cosine of the center-of-mass scattering angle ψ . The flux term gives

$$4\pi \int \frac{\omega d\omega}{(2\pi)^3} \mathbf{k} \cdot \frac{dN_m}{d\mathbf{x}} = \frac{I_2(m)}{I_1(m)} \hat{\mathbf{k}} \cdot \frac{dn}{d\mathbf{x}}, \quad (\text{A9})$$

where

$$I_r(m) = \int_0^m \frac{\omega^r d\omega}{e^{\beta\omega} - 1} \quad (\text{A10})$$

is the Debye integral and $\hat{\mathbf{k}}$ is a unit vector in the k direction. For the beam component we find

$$4\pi \int \frac{\omega d\omega}{(2\pi)^3} \xi_b \approx \frac{\lambda_2}{8\pi} h n_0 \frac{\delta(\theta)}{\sin\theta} \quad (\text{A11})$$

and

$$4\pi \int \frac{\omega d\omega}{(2\pi)^3} \mathbf{k} \cdot \frac{dN_0}{d\mathbf{x}} = \frac{I_2(\infty)}{I_1(\infty)} \hat{\mathbf{k}} \cdot \frac{d}{d\mathbf{x}} \left[h \frac{\delta(\theta)}{\sin\theta} \right]. \quad (\text{A12})$$

By equating the flux and scattering terms we arrive at the simplified form of the Boltzmann equations (45) and (46), with the scattering lengths

$$\kappa_1 = \frac{\lambda_1^2}{8\pi} \frac{I_1(m)}{I_2(m)}, \quad (\text{A13})$$

$$\kappa_2 = \frac{\lambda_1^2 \pi}{96\zeta(3)} \beta. \quad (\text{A14})$$

APPENDIX B

For the same scalar field interactions that were considered in Appendix A, the medium will thermalize if the self-interaction given by λ_2 is much larger than the scattering out of the medium given by λ_1 . In this case the Boltzmann equations (38) again take a simple form. The occupation number of the medium at a temperature β^{-1} will be approximately

$$N_m = \frac{1}{e^{\beta\omega} - 1}, \quad (\text{B1})$$

$$N_b = \frac{12\beta_h^2 h}{e^{\beta_h \omega} - 1} \frac{\delta(\theta)}{\sin\theta}, \quad (\text{B2})$$

where $12\beta_h^2 h \ll 1$. We can again take the occupation numbers of the untrapped modes to be negligible far from the hole. The scattering integral (A3) is given by

$$\begin{aligned} \xi = \int dk_1 dk_2 dk_3 (2\pi)^4 \delta(k_2 + k_3 - k - k_1) \\ \times \{ -\lambda_1^2 N_m(k) N_m(k_1) \\ - \lambda_2^2 N(k) N(k_1) [1 + N(k_2)] [1 + N(k_3)] \\ + \lambda_2^2 [1 + N(k)] [1 + N(k_1)] N(k_2) N(k_3) \}. \end{aligned} \quad (\text{B3})$$

The first term has the same form as the nonthermal case in Appendix A and gives the same result (A7). We can expand the remainder for small N_b to give

$$\xi = -\frac{\lambda_1^2}{4\pi} n(\mu) n_0 + \xi_m + \xi_b, \quad (\text{B4})$$

where

$$\begin{aligned} \xi_m = \lambda_2^2 \int dk_1 dk_2 dk_3 (2\pi)^4 \delta(k_2 + k_3 - k - k_1) \\ \times \left[12\beta_h^2 h(r) N_m(k) N_m(k_1) \right. \\ \left. \times N_m(k_3) e^{\beta\omega} \frac{e^{\beta\omega_1} - 1}{e^{\beta_h \omega_1} - 1} \frac{\delta(\theta_1)}{\sin\theta_1} \right], \end{aligned} \quad (\text{B5})$$

$$\begin{aligned} \xi_b = \lambda_2^2 \int dk_1 dk_2 dk_3 (2\pi)^4 \delta(k_2 + k_3 - k - k_1) \\ \times \left[12\beta_h^2 h(r) N_m(k_1) N_m(k_2) \right. \\ \left. \times N_m(k_3) e^{\beta\omega_1} \frac{e^{\beta\omega} - 1}{e^{\beta_h \omega} - 1} \frac{\delta(\theta)}{\sin\theta} \right]. \end{aligned} \quad (\text{B6})$$

For $\beta \approx \beta_h$, we take the frequency average to get

$$4\pi \int \frac{\omega d\omega}{(2\pi)^3} \xi_m = h(r) n_0 \lambda_2^2 f(\theta), \quad (\text{B7})$$

$$4\pi \int \frac{\omega d\omega}{(2\pi)^3} \xi_b = h(r) n_0 \lambda_2^2 f(\theta) \frac{\delta(\theta)}{\sin\theta}, \quad (\text{B8})$$

where $f(\theta)$ is a purely numerical function,

$$\begin{aligned} f(\theta) = \frac{9}{4\pi^5} \int x dx \int x_1 dx_1 \int d\bar{\mu} (e^x - 1)^{-1} (e^{x_2} - 1)^{-1} \\ \times (e^{x_3} - 1)^{-1} e^x \end{aligned} \quad (\text{B9})$$

and $x_2 = \beta\omega_2$, $x_3 = \beta\omega_3$ are determined by momentum conservation.

The frequency-averaged flux terms have the same form as given in Appendix A. If we replace $f(\theta)$ by a constant, we arrive at the simplified version of Boltzmann's equation (45) and (46) with $\kappa_1 = C\beta_1$, $\kappa_2 = \kappa_3 = C_2\beta$ where

$$\begin{aligned} C = \frac{\pi\lambda_1^2}{48\zeta(3)} f(0), \\ C_2 = \frac{\pi^2\lambda_2^2}{12\zeta(3)} f(0). \end{aligned} \quad (\text{B10})$$

Alternatively, if $\beta_h < \beta$, we can take the $\omega \ll \beta_h^{-1}$ limit in (B5) to give $\beta^{-1}\kappa_2 = \beta_h^{-1}\kappa_3 = C_3\beta_h^{-1}\beta$ where C_3 is another constant of order λ_2^2 . This corresponds to the fact that the number of particles scattered from the beam to the medium equals the number scattered from the medium to the beam.

¹S. Weinberg, Phys. Rev. D **9**, 3357 (1974); L. Dolan and R. Jackiw, *ibid.* **9**, 3320 (1974).

²S. W. Hawking, Nature **248**, 30 (1974); Commun. Math. Phys. **43**, 199 (1975).

³P. W. Higgs, Phys. Lett. **12**, 132 (1964); G. Guralnik, C. R. Hagen, and T. W. B. Kibble, Phys. Rev. Lett. **13**, 585 (1964).

⁴S. W. Hawking, Commun. Math. Phys. **80**, 421 (1981).

⁵D. J. Gross, P. D. Pisarski, and L. G. Yaffe, Rev. Mod. Phys. **53**, 43 (1981); D. J. Gross and F. Wilczek, Phys. Rev. Lett. **30**, 1343 (1973); S. Weinberg, *ibid.*, **31**, 494 (1973).

⁶P. Candelas, Phys. Rev. D **21**, 2185 (1980).

⁷M. Fawcett and B. Whiting, in *Quantum Gravity*, edited by C.

- J. Isham and M. J. Duff (Cambridge University Press, Cambridge, 1982).
- ⁸W. G. Unruh, *Phys. Rev. D* **14**, 870 (1976).
- ⁹J. B. Hartle and S. W. Hawking, *Phys. Rev. D* **13**, 2188 (1976).
- ¹⁰B. Carter, G. W. Gibbons, D. N. C. Lin, and M. J. Perry, *Astron. Astrophys.* **52**, 427 (1976).
- ¹¹D. N. Page, *Phys. Rev. D* **13**, 198 (1976).
- ¹²H. Georgi and S. L. Glashow, *Phys. Rev. Lett.* **32**, 438 (1974).
- ¹³M. Rees, *Nature* **226**, 333 (1977).
- ¹⁴S. W. Hawking and G. F. R. Ellis, *The Large Scale Structure of Spacetime* (Cambridge University Press, Cambridge, 1973).
- ¹⁵S. Coleman, *Phys. Rev. D* **15**, 2929 (1977).
- ¹⁶E. M. Lifshitz and L. P. Pitaevskii, *Statistical Physics* (Pergamon, New York, 1980).
- ¹⁷B. S. DeWitt, *Phys. Rep.* **19C**, 295 (1975).
- ¹⁸D. N. Page (private communication).
- ¹⁹S. Coleman and E. Weinberg, *Phys. Rev. D* **7**, 1883 (1973).
- ²⁰A. D. Linde, *Phys. Lett.* **108B**, 389 (1982).
- ²¹A. Chodos, R. L. Jaffe, K. Johnson, C. B. Thorn, and V. F. Weisskopf, *Phys. Rev. D* **9**, 3471 (1974).
- ²²R. Friedberg and T. D. Lee, *Phys. Rev. D* **16**, 1096 (1977).
- ²³C. Itzykson and J. B. Zuber, *Quantum Field Theory* (McGraw-Hill, New York, 1980).
- ²⁴G. W. Gibbons (private communication).
- ²⁵G. F. Chapline, *Nature* **253**, 251 (1975); B. Carr, *Astrophys. J.* **206**, 8 (1976).
- ²⁶C. E. Fitchel, D. A. Kriffen, and R. C. Hartman, *Astrophys. J. Lett.* **186**, L99 (1973).
- ²⁷I. G. Moss, *Nucl. Phys.* **B238**, 436 (1984).